

Embedded fiber-optic sensors in reinforced concrete beams for post event structural assessment

Original

Embedded fiber-optic sensors in reinforced concrete beams for post event structural assessment / Domaneschi, Marco; Cimellaro, GIAN PAOLO; Ansari, Farhad; Marasco, Sebastiano. - ELETTRONICO. - (2019), pp. 1-7. (ANIDIS 2019 - L'Ingegneria Sismica in Italia Ascoli Piceno 15 settembre 2019 – 19 ottobre 2019).

Availability:

This version is available at: 11583/2818638 since: 2020-05-01T16:44:59Z

Publisher:

ANIDIS - L'Ingegneria Sismica in Italia

Published

DOI:

Terms of use:

This article is made available under terms and conditions as specified in the corresponding bibliographic description in the repository

Publisher copyright

(Article begins on next page)



Distributed Measurements in Reinforced Concrete Beam

Marco Domaneschi^a, Gian Paolo Cimellaro^a, Farhad Ansari^b, Sebastiano Marasco^a

^a Department of Structural, Geotechnical and Building Engineering, Politecnico di Torino, Italy

^b Department of Civil and Materials Engineering, University of Illinois at Chicago, USA

Keywords: Fiber/optic sensors, RC beams; crack detection; image correlation.

ABSTRACT

Reinforced concrete structural components are subjected during their service life to different loading conditions that may affect their durability and efficiency. This can reduce the safety level of the structure over the time until it degrades completely up to its ultimate limit state. In particular, reinforced concrete elements can develop cracking due to seismic loading leading to the exposure of the reinforced concrete elements to the aggression of external agents. Therefore, their post-earthquake structural assessment can be a procedure of great interest to ensure the durability and efficiency of existing reinforced concrete structures, especially when important and strategic buildings and infrastructural systems are considered. Being able to monitor the development and evolution of cracking may be crucial and this research is aimed at this purpose. In particular, laboratory tests are described on reinforced concrete beams equipped with distributed fiber optics sensors to monitor the state of cracking and its thickness propagation. The main objectives of the research can be summarized as (i) deformation and temperature development from concrete casting, (ii) crack detection and localization with distributed FOS, (iii) comparing sensing cables design and digital image correlation procedures.

1 INTRODUCTION

Fiber Optic Sensors – FOS – have several important attributes as well as geometric adaptability, immunity to electrical and magnetic interference, high resolution that make them excellent in Civil Engineering field to detect anomalies and cracks but also in dynamic conditions to assess structural characteristics as modal parameters (Ansari 2007, Casciati et al. 2005, Domaneschi et al. 2017). The great advantages of FOS over traditional sensors have led to them being considered as an important technology in structural monitoring. The sensing crack-induced strains in the distributed sensors from frequency shift can be used to investigate damage conditions in civil structures.

In this work, laboratory tests are described on reinforced concrete beams equipped with distributed fiber optics sensors to monitor the state of cracking and the propagation in the thickness.

1.1 Test design

The reinforced concrete beam is designed to have a ductile behaviour in order to follow the crack growth, being one of the goals of this study

the localization of the crack so in order to get this objective it is very important to have a gradual propagation of crack. The cross section of the beam is 150 mm wide and 300 mm high. The longitudinal reinforcement is composed by two bars of 14 mm of diameter in compressive zone and two bars of 18 mm of diameter in tensile zone. There are stirrups of 8 mm of diameter as shear reinforcement that are spaced with 70 mm from the bearing to 500 mm and from this point they are spaced with 140 mm (Fig.1). The following two materials are selected: C 25/30 and B450C.

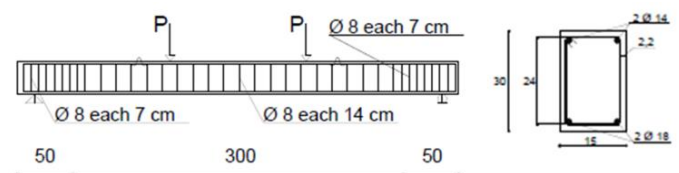


Figure 1. Reinforced Concrete beam details.

On the tensile surface, there are two notches that are created to initiate cracks in a decided location. The notches are designed at 1550 mm from the bearing but during the installation of the

crack initiators, the one on left side is put a 1600 mm. Four-point bending test is performed, the distance between the two points of loads application is 1230 mm (Fig. 2).

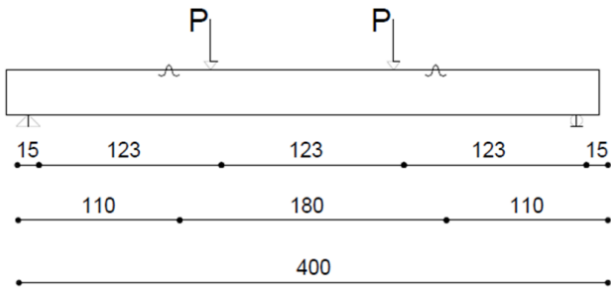


Figure 2. Four point bending test scheme.

2 SENSOR POSITIONING

2.1 Installation

Five types of FOS are embedded, four are strain sensors and one is temperature sensor (Fig. 3)

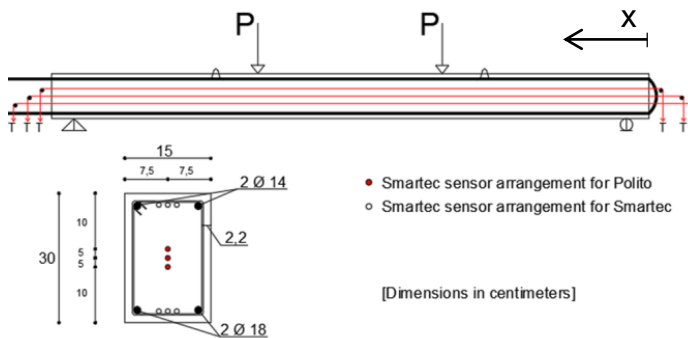


Figure 3. Sensors positioning.

Because of laboratory problem, it is impossible to install three separate sensors, so there is one that go inside of the central part of the beam three time. During the installation of the embedded sensors, those ones that were not glued to the steel rebars and parallel to the beam axis (red lines in Fig. 3), an issue occurred. At a certain X distance from the right end section of the beam, the middle and the bottom sensors crossed themselves two times. In other words, in that position they were not parallel but coincident. Externally there are four types of distributed sensors, two of them are completely different from the embedded sensors (Fig.4).



Figure 4. Distributed sensors scheme.

FBG sensors are applied in the middle span glued on the tensile and compressive rebars.

Comparing the results collected from FOS and FBG, according to the objectives of the test, it should be possible to get the performance of distributed sensors. Flexpatch system is glued on the frontal surface of the beam. This is a Monitoring Wireless System that is composed by strain sensor, thermometer, tilt sensor, seismographic sensor and transmission unit. Behind, on the opposite side there is another system to control strain and cracks: Digital Image Correlation. The beam is painted of white from the middle span to 500 mm on each side, there are dots drawn on the paint. A camera captures the distance changes between the dots at each loading step. Clip gauge extensometer and Linear Variable Differential Transformer are applied on the beam in order to measure the deflection and the crack opening at the notches locations (Fig. 5).

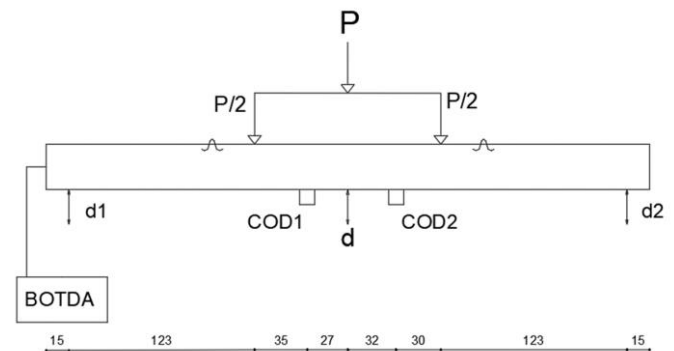


Figure 5. LVDT arrangement.

3 LOAD TEST

3.1 Four-point bending test

It is performed a test on 4 cubes in order to estimate the compressive strength of the concrete used for the beam. The cubes have a side of 150 mm, the results obtained are show in the Table 1.

Table 1. Compressive strength of cubes.

Specimen No.	[kN]
1	550
2	600
3	449
4	573

A steel beam distributes the load coming from the piston on two points, the stroke of the piston is controlled by displacement.

The cracking load is around 10 kN against the 7 kN of the design (Fig. 6), it sounds a good result because the design properties of materials are affected by the coefficient of the NTC 2018 (the Italian code for civil construction). The bending load and the ultimate load present differences between the design and the real value

due to the same reason. It is important to know that for the design value, the confinement effect of the stirrups is taken into account. During the test, the behavior of the beam is extremely ductile, as predicted by the project, so that it is possible to capture the progressive growth of the cracks. At the end of the test there are two types of cracks: one due to bending moment and the other due to shear. It is possible to see vertical cracks between the two loading points where only the moment acts, while cracks at 45° between the support and the loading point, area in which the shear intervenes (Fig. 7).

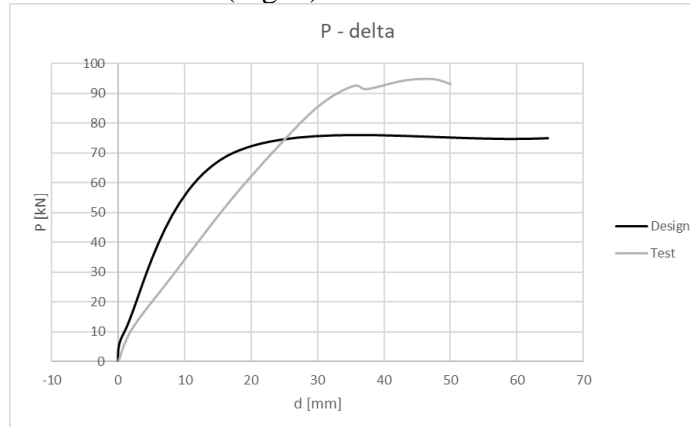


Figure 6. Comparison between design and test force-displacement relationship.



Figure 7. Cracks on tested beam.

4 MEASUREMENTS DURING CURING AND POSITIONING ON THE SUPPORTS (SELF-WEIGHT)

4.1 Temperature sensor

As mentioned above, one of the embedded sensors measures the temperature change. The initial setting phase of the concrete is known to be exothermic, distributed change in temperature during strength development in concrete is expected. Starting from first placement of fresh

concrete in the form for a period of 18 hours, the Fig. 8 shows the Brillouin frequency change over the length of the temperature sensors over the span length of the beam.

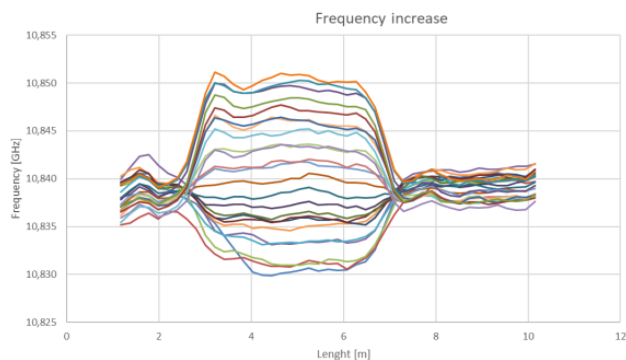


Figure 8. Brillouin frequency change.

The change in frequency is measured over a length of 8,9 m, from 1,17 m to 10,15m, but the real length of the embedded temperature sensor is from 2,9 m to 6,9 m, that represents size of the beam. The Fig. 9 is the frequency change over a length of 8,9 m, but now it is plotted only the first and the last measurement.

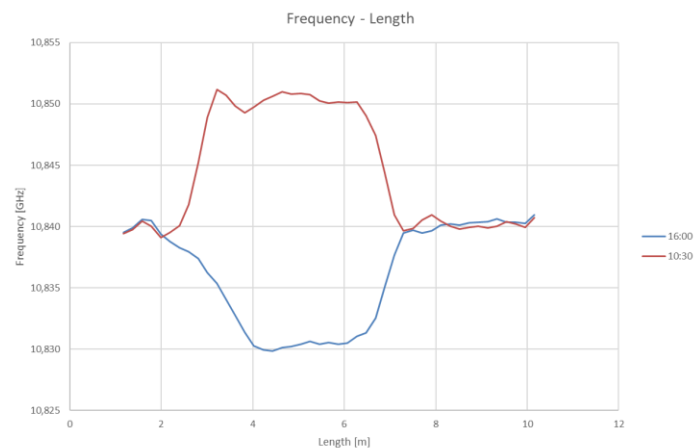


Figure 9. Frequency change over 8.9 m length.

From the first and last measurements it is clear to note an increase in frequency due to the increase in temperature following the curing of the concrete. The Fig. 10 is the temperature change over the length of the temperature sensors over the span length of the beam.

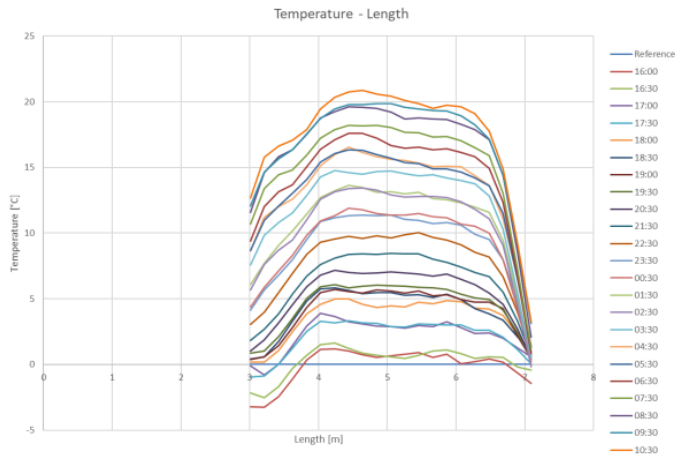


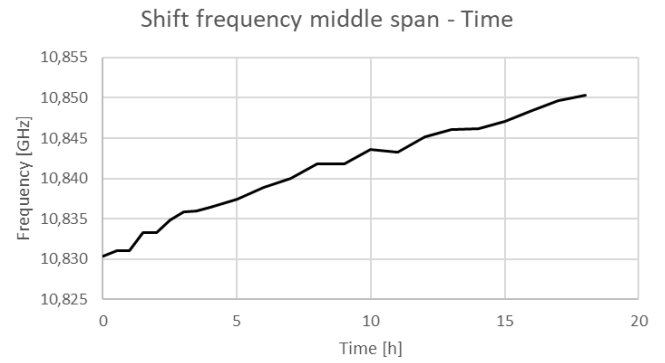
Figure 10. Temperature change over beam length.

In the first 18 hours a temperature increase of about 20° is calculated. A local calculation of the middle span point is carried out, so the shift in frequency of this point during the first 18th hours due to the Brillouin frequency change of the temperature sensors and the growth temperature in the same point during the first 18th hours due to change frequency of temperature sensor are plotted in the Fig. 11.

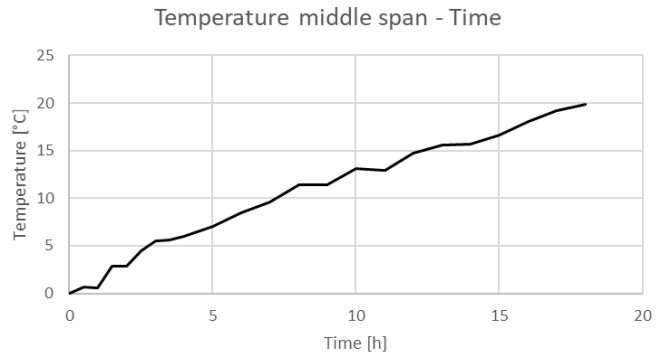
This measurement could be more accurate with an initial measurement of room temperature, it is clear that it is not possible to start from 0°C .

4.2 Strain due to the self-weight

As shown in Figure 3, the three embedded sensors should have been stretched to obtain optimal results in the calculation of deformations. Confirmation of this is obtained by calculating the deformations due to self-weight (Fig. 12).

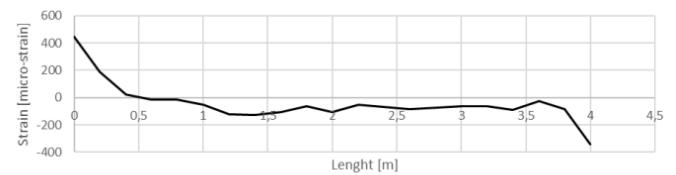


(a)

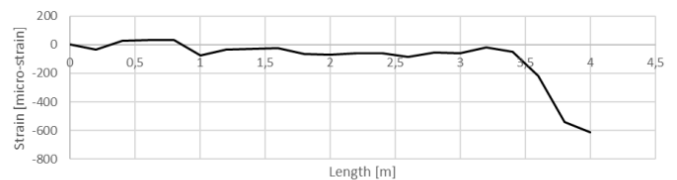


(b)

Figure 11. Frequency and temperature change over time.



(a)



(b)

Figure 12. Measured strain for top sensor (a) and bottom sensors (b).

5 MEASUREMENTS DURING THE FOUR-POINT BENDING TEST

5.1 Temperature sensor

During the test takes place a distributed change in temperature. Embedded distribute temperature sensor records a frequency variation probably due to the fact that the test lasted the whole day and therefore there was a daily temperature variation and also two powerful lights are installed for Digital Image Correlation

that may have contributed to raising the frequency.

5.2 Strain sensors

Embedded FOS not bonded to longitudinal reinforcement bars and external FOS are treated below. The authors want to capture in particular the movement of the neutral axis with the first three, while with the external authors realize that it is easier to guess the formation of a crack as far as possible having a Spatial Resolution of 0.5 m.

5.3 Embedded sensors

Fig. 13 shows the strain variation measured by the top sensor along the beam length during the test. Part of the top sensor remains in compression until very late stages of loading. This also indicates that the neutral axis is not symmetric during his moving.

Strain variation along the beam length during the test, it is possible to see the first and the last measurement of the top sensor, it is clear that the sensor has recorded this variation between tension and compression, which according to the authors is the result of two factors that may have occurred separately:

- movement of the neutral axis not symmetrical
- malfunction of the sensor due to incorrect installation of the same.

The Fig. 14 is a plot of the frequency change of the top sensor along the beam length during the test. The double humps in this sensor is due to the location of the two loads in the 4-point bend. However, they shift, indicating the effects of the multiple cracks within the SR measurements of the system.

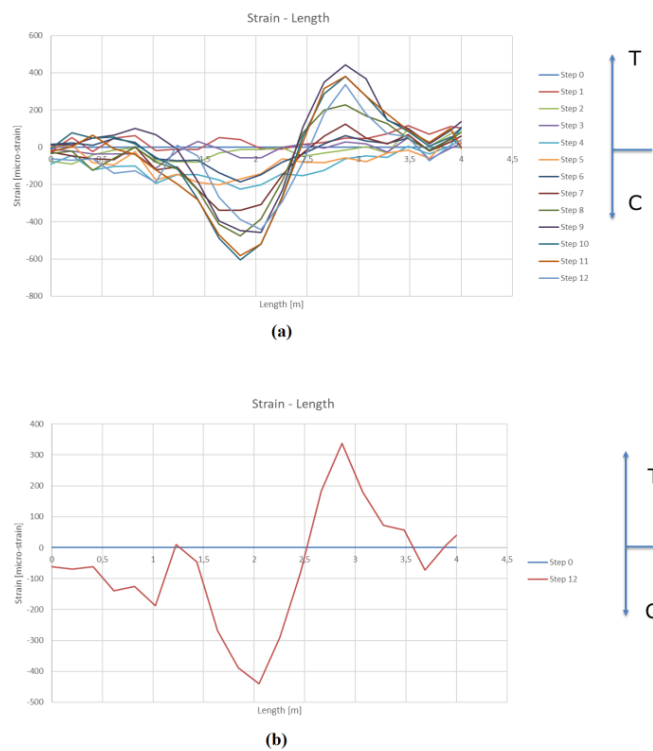


Figure 13. Strain variation measured by the top sensor.

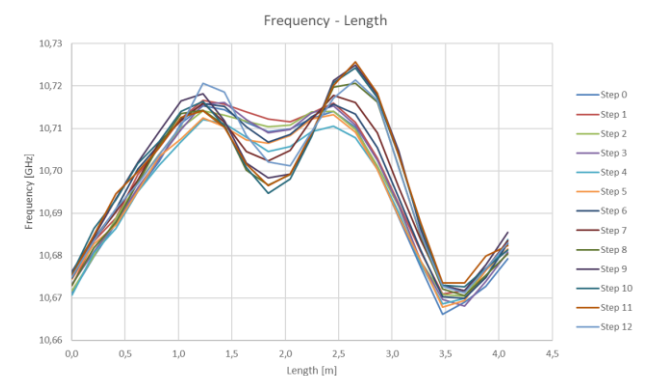


Figure 14. Frequency change of the top sensor along the beam length.

The analysis of the middle sensor gives the idea how the flexion of the beam increased during the test up to the formation of multiple cracks that are also witnessed by the large strains above 500 micro strain (Fig. 15).

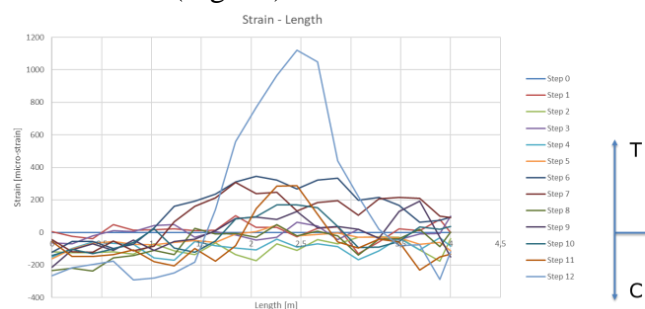


Figure 15. Strain variation over beam length.

The bottom sensor confirms the measurements of the middle one, with the trend of the strain

increases because the sensor is in the tensile part of the section along the beam.

5.4 External sensors

Externally there are 3 different types of sensors:

- H&G sensor
- SMART TAPE sensor
- SMART PROFILE sensor

The sensors are glued in total 4, because there are two SMART PROFILES one on the bottom of the beam and one on the top. The H&G sensor is glued on the bottom and the results of measurement confirm the common bending strain diagram due to the self-weight and the four-point bending test (Fig. 16).

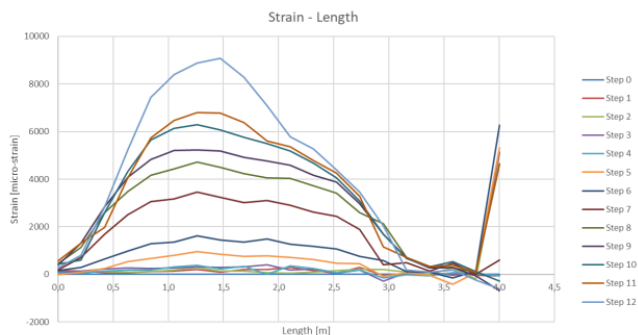


Figure 16. Strain variation over beam length.

The SMART TAPE sensor is the first to give the impression that it is possible to gather some information on the location of the crack despite the Spatial Resolution is very high for current technologies.

From Fig. 17 it is possible to see at different steps the onset of very high strains in some points. The SMART PROFILE sensor confirms the above and is considered to be the one with the greatest ability to pick up cracks.

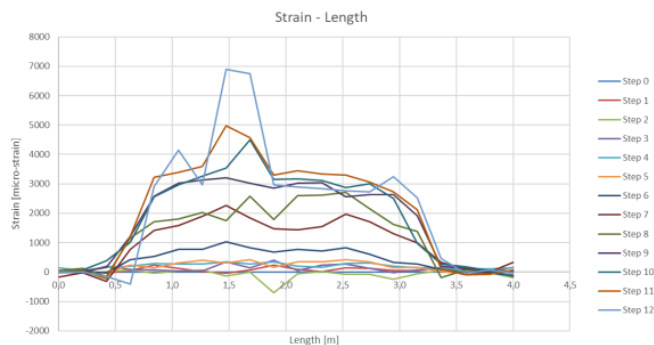


Figure 17. Strain variation over beam length.

6 COMPARISON BETWEEN SENSORS

6.1 FOS and Digital Image Correlation (DIC)

A comparison between FOS results with DIC ones can help to confirm some observed outcomes and highlight new

ones. A DIC computation is proposed in Fig. 18 that can help in locating the crack with FOS. The digital image correlation was performed in the central part of the beam, from 1,5m to 2,5m. It is possible to see as in the step number 7 of the test, the external SMART PROFILE sensor at 2,25 m shows an increase in frequency and in strain that matches the results obtained from the digital image correlation. Indeed, in this point at that step, a crack could be occurred and the variation in strain was so big.

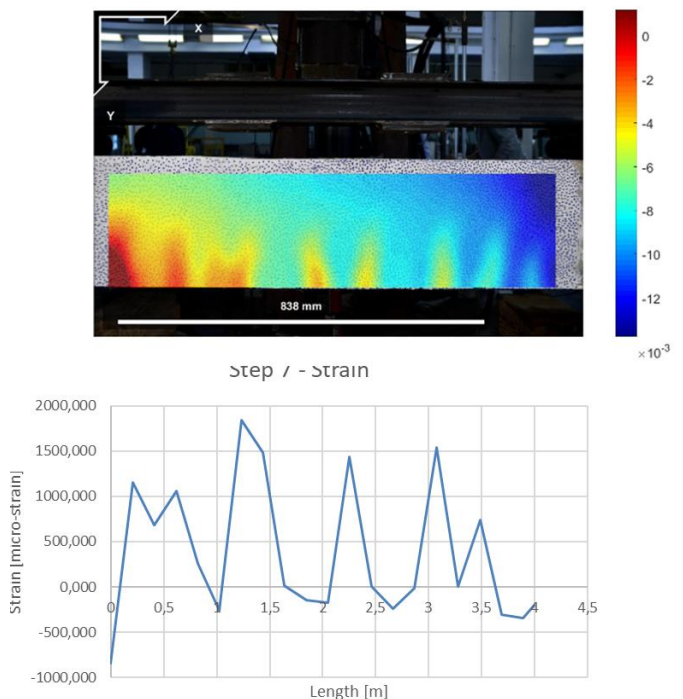


Figure 18. Comparison between FOS and DIC.

7 CONCLUSION

The implementations of embedded Fiber Optic Distributed Sensors in a reinforced concrete beam to assess the evolution of temperature and strain are described in this work. Different measurements have been considered with the aim to develop the potential of these sensors when embedded in concrete elements. Digital Image Correlation technique has been also considered during the tests for comparison with FOS. Even the low resolution implemented, the fiber optic measures have been able to highlight the

evolution of the beam conditions during the loading phase.

8 ACKNOWLEDGEMENTS

The research leading to these results has received funding from the European Research Council under the Grant Agreement n°ERC_IDEalreSCUE_637842 of the project IDEAL RESCUE - Integrated DEsign and control of Sustainable CommUnities during Emergencies.

The technical support of the MastrLab at Politecnico di Torino DISEG is also gratefully acknowledged.

REFERENCES

- Ansari, F. 2007. Practical Implementation of Optical Fiber Sensors in Civil Structural Health Monitoring, *Journal of Intelligent Material Systems and Structures*, **18**. DOI: 10.1177/1045389X06075760.
- Casciati, S., Domaneschi, M., Inaudi, D. 2005. Damage assessment from SOFO dynamic measurements, *Proceedings of SPIE - The International Society for Optical Engineering*, **5855**(258): 1048-1051. DOI: 10.1117/12.623656.
- Domaneschi, M., Sigurdardottir, D., Glišić B. 2017. Damage detection based on output-only monitoring of dynamic curvature in concrete-steel composite bridge decks, *Structural Monitoring and Maintenance*, **4**(1): 1-15.